Wildfires trigger multi-decadal increases in sedimentation rate and metal loading to subarctic montane lakes

Nicolas Pelletier [a], John Chételat [b*], Sarah Sinon [a] and Jesse C. Vermaire [a]

[a] Geography and Environmental Studies, Carleton University, Ottawa, ON K1S 5B6, Canada

[b] Environment and Climate Change Canada, National Wildlife Research Centre, Ottawa, ON K1A 0H3, Canada

*Corresponding author. Tel.: +1 613 991 9835; fax: +1 613 998 0458

Email address: john.chetelat@canada.ca (J. Chételat)

Keywords: erosion, remobilization, climate change, Yukon, mercury, lead

Highlights

- Lake sediment accumulation and metal concentrations increased after two wildfires.
- Mercury and lead fluxes to sediment increased dramatically in one of the lakes.
- The second fire was more impactful to a lake with a previously burned catchment.
- Lakes with minor catchment burns showed less or no impact on sediment metal fluxes.
- Severe fire burns increase catchment transport of metals to montane lakes.

Abstract

We evaluated how two large wildfires affected the sedimentation rate and accumulation of lead (Pb), mercury (Hg), and cadmium (Cd) in sediment of four subarctic montane lakes in the Yukon, Canada. The wildfires occurred 60 and 20 years (1958, 1998) before sediment collection in 2018. Site-specific fire exposure was inferred from the charcoal accumulation histories in the lake sediments and the burned catchment area was determined from historical fire maps. The two major wildfires caused a two to five-fold increase in sedimentation rates and a two to eight-fold increase in sediment metal accumulation rates in Little Fox Lake. The mass accumulation rates of metals in Little Fox Lake sediment increased by a maximum of 2.7–4.7 mg Pb m^{-2} yr^{-1}, 19–29 μg Hg m^{-2} yr^{-1} and 37–114 μg Cd m^{-2} yr^{-1} following wildfires. Modelling using elemental ratios of lithogenic sources suggested a large proportion of the Pb and Hg accumulating in post-fire sediment was from remobilized legacy anthropogenic pollution. In contrast, Cd fluxes were consistent with variation in catchment weathering. Impacts of wildfires were visible but more muted in the sediment of Little Braeburn Lake, whereas Fox Lake and Grayling Lake sediments showed little to no wildfire impact and served as a reference for external (long-range) metal deposition. Major changes to lake sediment geochemistry in Little Fox Lake were caused by the lack of vegetation and soil recovery in the catchment following the severe 1998 fire. Wildfire impacts were persistent in the lake more than 20 years after the last fire, with no sign of a return to pre-fire Pb, Hg, and Cd accumulation rates. This study shows that wildfires in northern montane catchments can significantly increase the rate of metal accumulation in affected lakes, thereby impeding recovery from reductions in anthropogenic air emissions of these metals.

1. Introduction

Wildfire occurrence and severity will increase in many regions, including northwestern Canada, in response to climate warming and the interplay between future precipitation and atmospheric

41 temperatures (Coogan et al., 2019; Krawchuk et al., 2009). The fire return interval is already short in
42 the southern Yukon (Canada) boreal forest, dominated by lodgepole pines (Prince et al., 2018), and
43 models predict an imminent increase in the annual burned area in the Yukon (Kitzberger et al., 2017).
44 In lakes near burned forests, the loading of particles and solutes to lakes following fires can increase
45 by the transport of ash, organic matter, and dissolved compounds via surface and groundwater flow
46 or atmospheric transport (Jensen et al., 2017). The post-fire transport of particulates can be especially
47 important during storm events (Burton et al., 2016; Filgueira and Vega, 2006; Shakesby, 2011) and in
48 montane areas with steep catchment slopes (Abbate et al., 2019; Evans et al., 2017; Meng et al., 2015).
49 The release (remobilization) of natural and legacy anthropogenic metals from catchment soils and
50 biomass by wildfire has been observed in lake sediment (Odigie et al., 2015; Odigie and Flegal, 2014),
51 fly ash samples (Isley and Taylor, 2020; Wu et al., 2017) and soils following controlled burn (Abraham
52 et al., 2018). Yet, there is still limited information to help with the prediction of future impacts of
53 wildfires on the accumulation rates of metals in lakes, particularly in subarctic regions. This study
54 investigated the loading of ecotoxicologially relevant metals [mercury (Hg), lead (Pb), and cadmium
55 (Cd)] in four subarctic lakes to help constrain the possible impacts of a future increase in subarctic
56 wildfire frequency and intensity.

57 The impact of burned catchments on boreal lake geochemistry typically lasts two to three decades
58 (Dijkstra et al., 2013; Dunnette et al., 2014), and includes greater loading of terrestrial organic matter
59 (Dunnette et al., 2014; Leys et al., 2016; Pompeani et al., 2020), nutrients (especially phosphorus)
60 (Paterson et al., 2002; Philibert et al., 2003; Waters et al., 2019), and metal(loid)s (Abraham et al., 2017).
61 These changes can have ecological consequences for aquatic organisms, including invertebrates
62 (Garcia et al., 2007; Harper et al., 2019; Pretty et al., 2020) and fish (Garcia and Carignan, 2005; Kelly
63 et al., 2006; Spencer et al., 2003). However, the impact of wildfires on lake geochemistry should vary
64 by physiographic region according to vegetation, hydrology, soil, and topography (Harper et al., 2019;

Pereira and Úbeda, 2010; Pompeani et al., 2020; Shakesby, 2011). The burn conditions, including fuel load, fire severity, and extent, may also modulate the impact of wildfires on lake geochemical fluxes and the reactivity of the elements released by wildfires (Cerrato et al., 2016; Webster et al., 2016). More intense wildfires burn at higher temperatures and consume more plant biomass and organic soils, therefore mobilizing a greater quantity and a more comprehensive range of elements (Bodí et al., 2014; Campos et al., 2015; Kohlenberg et al., 2018; Nzihou and Stanmore, 2013). Because many factors are involved in the magnitude and duration of wildfire impacts to local freshwaters, studies done on a wide range of geophysiographical regions, vegetation type, topography, burn extent and burn severity will be necessary to obtain an accurate global estimate of future freshwater contaminant loading from wildfires. In this study, we focused on the cordilerian region of the Yukon as it is an environment with severe and frequent wildfires and high gradient slopes, which we hypothesised would lead to large catchment erosion fluxes following wildfires.

Severe wildfires may surpass ecological thresholds preventing the recovery of soils and vegetation (McLauchlan et al., 2020; Stevens-Rumann and Morgan, 2019). For example, a short fire-return interval of severe wildfires can inhibit the regeneration of subalpine lodgepole pine (*Pinus contorta* Douglas) forests (Turner et al., 2019) and subarctic black spruce (*Picea mariana* Miller) forests (Brown and Johnstone, 2012). Most paleolimnological analyses of wildfires in lake sediment have looked at the impact of fires over the Holocene, with little distinction between ancient fires and recent ones (e.g., Dunnette et al., 2014; Pelletier et al., 2020). Since the geochemical cycling of metal(loid)s has been disturbed by human activities, particularly during the 20th century, analyses of recent wildfire impacts may stand out from impacts measured from ancient wildfires, particularly those preceding the Industrial Revolution (ca. 1850). It is for this reason that we focused on wildfires occurring in the last

88 ~100 years. This is a period for which it is easier to obtain an accurate sediment chronology (from
89 ^{210}Pb) and that is underrepresented in wildfire reconstructions from natural archives, which often
90 focus on long-term fire frequency and requires the observation of a large number of events to make
91 statistical inferences.

92 We measured the impacts of two large wildfires, which occurred approximately 20 and 60 years ago,
93 on sedimentation rates and metal loading in four lakes located 50-80 km from Whitehorse, Yukon,
94 Canada. A large section of one lake's catchment (Little Fox Lake) has never recovered ecologically
95 from the most recent wildfire events. Thus, this study provided a rare opportunity to examine the
96 long-term (decadal) impacts of a severe stand-replacing wildfire on lake sediment geochemistry. This
97 research is needed in the current context where major fire events exceeding the threshold for
98 ecological recovery are predicted to become more frequent in future years. We chose the cordilerian
99 region of the Yukon for this study since it is an environment with severe and frequent wildfires and
100 high gradient slopes, which we hypothesised would lead to large catchment erosion fluxes following
101 wildfires.

102 **2. Methods**

103 **2.1 Study area**

104 The study lakes were Fox Lake, Little Fox Lake, Grayling Lake (unofficial name) and Little Braeburn
105 Lake, all located within the Yukon Boreal cordillera, along the Klondike Highway (Yukon Highway
106 2). The valley comprising all lakes is underlaid by a fault between a sedimentary terrane from the
107 Tanglefoot formation and a sedimentary/volcanic terrane from the Nordenskiold, both from the
108 Laberge group (Colpron, 2011). Predominant trees species near the study lakes where white spruce
109 (*Picea Glauca* (moench) voss), trembling aspen (*Populus tremuloides* Michx.), and lodgepole pine (*Pinus*
110 *contorta* Douglas). The yearly average temperature at the closest weather station (Takhini River Ranch,

35-60 km south) is -1.4°C, with 228 mm of annual precipitation of which 72 mm is snow (ECCC, 1981-2010). Minimum temperatures occur in January (mean = -18.2°C) and maximum temperatures occur in July (mean = 13.9°C). Snowmelt usually occurs in March-April with a maximum yearly snowdepth of 41 cm (ECCC, 1981-2010). The lake catchments have a moderate to steep topography, with average slope gradients of 7-12% for Little Braeburn Lake, flat for Grayling Lake, 13-19% for Fox Lake, and 23-32% for Little Fox Lake. The approximate maximum water depth in the study lakes, obtained from a hand-held sonar and commercial bathymetric maps, was 45 m for Fox Lake, 35 m for Little Braeburn Lake, 25 m for Little Fox Lake, and 6 m for Grayling Lake.

2.2 Historical wildfire activity in the study area

Severe fires occurred in the study area in 1958 (1342 km^2 burned) and 1998 (439 km^2 burned) (Figure 1) (Yukon Wildland Fire Management, 2014). Vegetation has minimally recovered from the 1998 fire, and the thick organic soil layers found in unburned areas offer a striking contrast with the bare mineral soils in adjacent burned slopes (Figure 2). The catchments of each study lake were affected to a varying degree by the 1958 and 1998 fires (Supplementary Table S1). All of the Little Braeburn Lake catchment was affected by the 1958 fire but was untouched by the 1998 fire. Fire maps indicated that the Little Braeburn catchment was burned up to the shore by the 1958 fire (Figure 1). However, the field investigation revealed no ash layer directly around the lake, suggesting that a buffer of soil and vegetation around the lake may have remained after the fire. Previous investigations of the 1958 wildfire have reported an uneven stand-age structure following the fire, indicating a low-intensity fire (Marcantonio, 2007). The Little Fox Lake catchment was partially affected by the 1958 fire (42% of the catchment area) and almost entirely affected by the 1998 fire (99% area), including a 159 km^2 area that burned twice over the 20 years. There were signs of fire directly around the lakeshore, including ash and charcoal in the nearby soil profiles. The Fox Lake catchment was only partially affected by the 1958 and 1998 fires (43 and 20% of the area burned, respectively), and most of the lakeshore

remained untouched by both fire events. Previous investigations of fire history in the area based on dendrochronology and lake sediment analysis revealed severe wildfires in ca. 1760, 1775, 1835, and 1920 (Marcantonio, 2007).

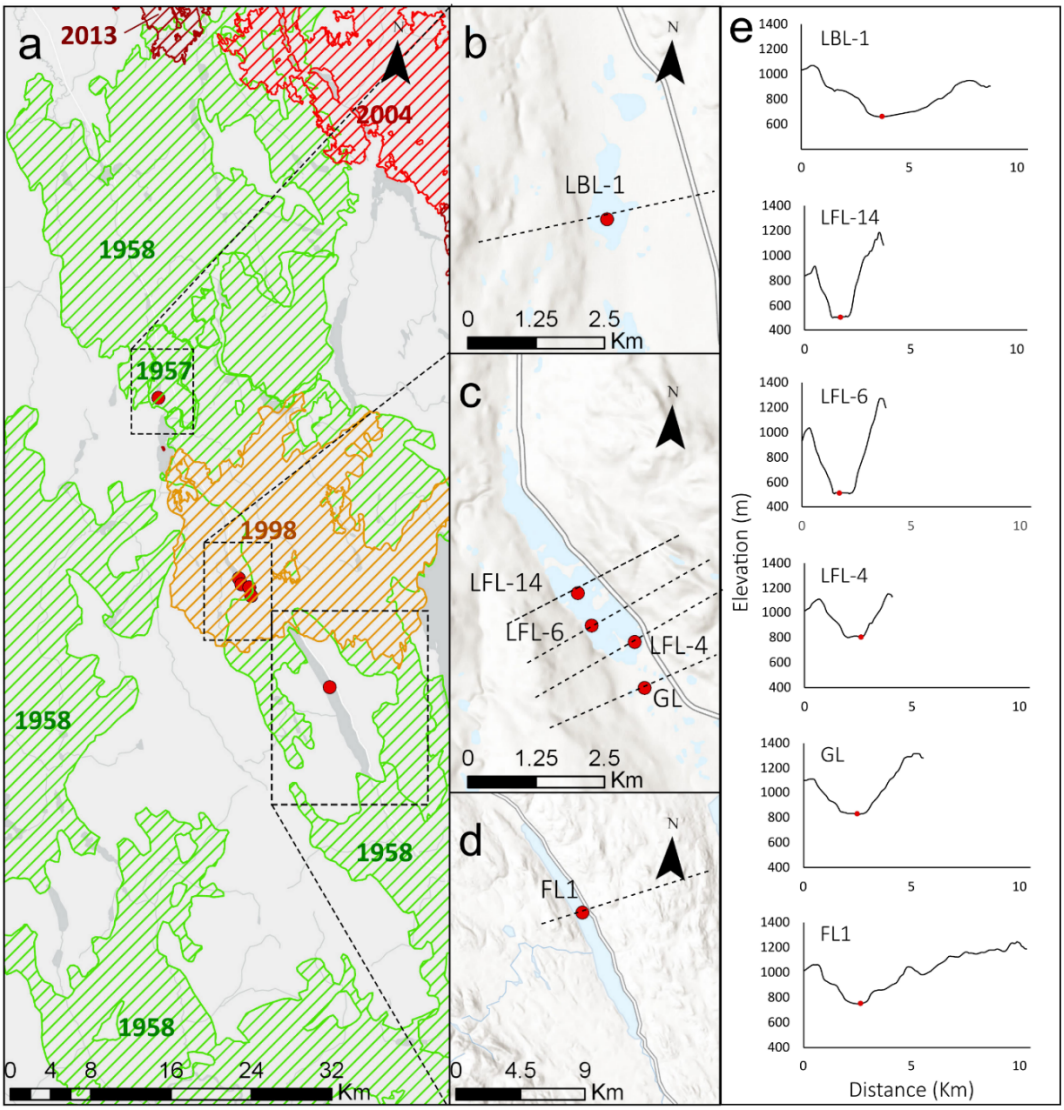

Figure 1: (a) Locations of lake sediment cores collected in 2018. The colored polygons are the wildfire scars with the year of the fire event indicated (Wildland Fire Management, 2014). (b, c and d) Close-up view of the lakes with shading showing the surrounding topography. The individual maps are showing Little Braeburn Lake (b), Little Fox Lake and Grayling Lake (c), and Fox Lake (d).The dashed

lines indicate the orientation of the cross-sections presented to the right . (e) Topographic cross-section of the valley at the sampling locations for each lake sediment core.

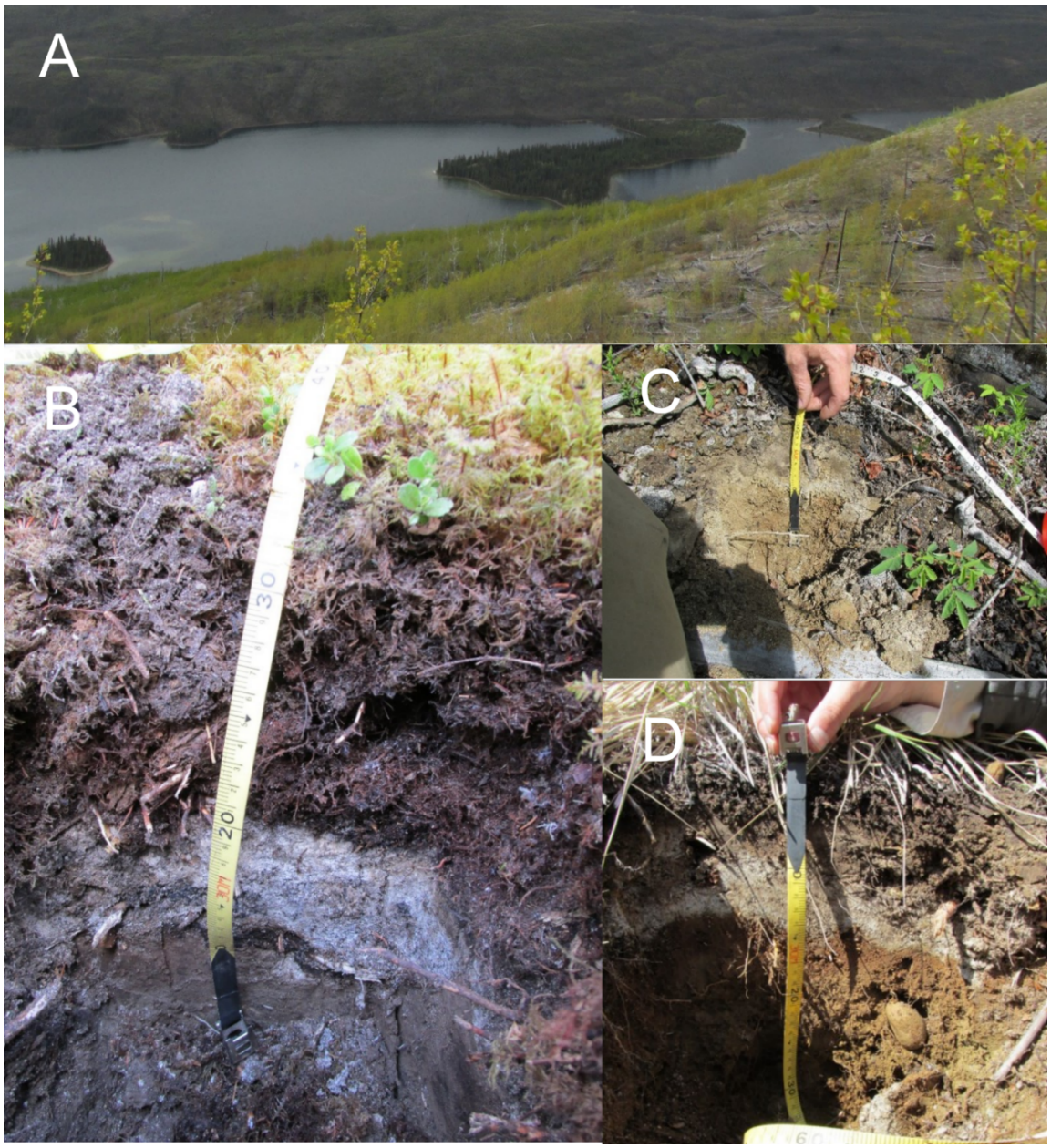

Figure 2: (a) View of the east and west sides of the Little Fox Lake catchment: the east side (bottom of the picture) burned twice and had little vegetation cover 20 years after the second fire event; the west side (top of the picture) burned in 1958 and vegetation recovery was evident; (b) thick (>15 cm) organic soil layer with a moss cover at the bottom of a slope that burned once in 1958; (c and d) thin

organic soil layer (~5 cm) at the bottom of a slope burned twice in 1958 and 1998 near Little Fox Lake.

2.3 Sampling procedures

Sediment cores were collected from a canoe in July 2018 using a UWITEC gravity corer. Cores were collected from the deepest sections of each lake based on a handheld depth finder. Six of these cores from four different lakes were selected for analysis. We selected the cores from each lake that were longest and most undisturbed based on the appearance of the sediment-water interface at the time of collection. Analyzed core lengths varied between 20.5 and 33 cm. Sediments were extruded from the core tubes on the same day they were recovered from the lake and sliced into 0.5 cm increments except for the uppermost slice at the sediment-water interface, which was a 1 cm interval. Sediment samples were placed in Whirl-pak bags and weighed to obtain wet weights. Sediment samples were frozen in the field and shipped back to Carleton University, Ottawa, Canada, where they were kept at 4 °C until further processing. At Carleton University, a 1 cm^3 sub-sample of homogenized sediment from each interval of the cores was set aside for charcoal analysis. The remaining sample material was freeze-dried and weighed again to obtain dry weights. Sediment density was calculated from the dry weight of the sediment divided by the volume of the sample, taking into consideration the 1 cm^3 previously removed for charcoal analysis.

2.4 Charcoal analysis

The 1 cm^3 fresh sub-samples set aside for charcoal analysis were treated in 11% sodium hypochlorite at room temperature for 24h to make charcoal particles more distinguishable from mineral and uncharred organic matter. The solution was then filtered with a 150 μm mesh to remove smaller particles and retain macroscopic charcoal. The sediments coarser than 150 μm were carefully distributed on the mesh to avoid overlapping of particles and photographed with a Leica Si9 dissection

microscope using the LAS EZ (Leica®) software at a magnification of six times. Photos were then analyzed using *Image J* software (Rasband, 1997-2018) to determine the count and surface area of charcoal in each sample. Within *Image J*, the image brightness was manually adjusted to ensure that the charcoal was recognized by the software and distinguished from any remaining uncharred organic matter. The charcoal of each sub-sample was quantified based on three characteristics: abundance (#/cm^3), cumulative area (mm^2/cm^3), and mean size of charcoal (mm^2/ unit). The mean charcoal size was determined by dividing the cumulative area by charcoal abundance of the subsample. Before any image analysis, *Image J* was calibrated to the scope resolution (mm/pixel) using a 0.5 mm diameter machined pencil lead.

2.5 Core chronologies

Chronologies for the sediment cores were developed using radiogenic lead (^{210}Pb) and the Constant Rate of Supply (CRS) model (Appleby and Oldfield, 1978). The ^{210}Pb activity was measured by alpha spectrometry in 12-15 sediment slices per core. The ^{210}Pb activity in sediment layers was interpolated following a log-linear relationship with cumulative dry sediment weight (g cm^{-2}). We used the mean of two to four measurements of ^{226}Ra activity by alpha spectrometry per core to estimate the supported ^{210}Pb activity in the sediment core. Measurements were conducted at Flett Research Ltd (Winnipeg MB, Canada). Activity profiles of ^{210}Pb and ^{226}Ra for each sediment core are provided in the supplementary information (Figure S1).

2.6 Geochemical analysis

Freeze-dried sediments were digested by aqua regia and analyzed for concentrations of 37 elements by ICP-MS following the Bureau Veritas Minerals (BVM) method AQ250. The dry sediment samples were also analyzed for Hg concentration in four cores using a Direct Mercury Analyzer (DMA). DMA measurements were conducted on a DMA-80 Evo Direct Mercury Analyzer (Milestone Inc., CT,

196 USA) on freeze-dried samples without prior digestion. The Hg concentrations in cores LFL-14 and
197 LFL-6 were obtained with ICP-MS measurements only at BVM. We compared ICP-MS and DMA
198 measurements for Hg in the four cores where both measures were obtained to ensure comparability
199 between results (see spreadsheet in the supplementary material). The sediment Hg concentrations
200 measured by both analyses (n=103) had 6±4% RSD (mean ± standard) between methods, and the
201 differences in concentrations between methods were not significantly different (paired t-test, p=0.78).
202 A complete QA/QC analysis comprising the measurement of analytical blanks (n=6), sediment
203 samples duplicates (n=5), standard reference material (n=8), and in-house standards (n=12) is
204 presented for each analyzed element in spreadsheets included in the supplementary material.

205 **2.7 Modelling of lithogenic and anthropogenic Pb, Hg, and Cd in the sediment**

206 To model changes in metal sources, we assumed that in preindustrial sediments, Pb and Cd loadings
207 were entirely derived from catchment erosion and that Hg was derived from a combination of
208 catchment erosion and organic matter accumulation. A Spearman rank order correlation analysis of
209 Hg concentration and organic matter content was carried out for each core to determine if changes in
210 Hg accumulation were likely to be primarily caused by changes in organic matter accumulation. The
211 significance level for this analysis was $p<0.05$. In agreement with previous observations in other lakes
212 (Feyte et al., 2010, 2012; Sanei et al., 2010; Sanei and Goodarzi, 2006), organic matter influences were
213 included because of strong correlations between sediment percent organic matter and Hg
214 concentrations. We modeled the contributions of Pb and Cd from lithogenic sources in modern (post-
215 1850) sediments using the ratio between the element of interest and a conservative lithogenic element
216 [Aluminum (Al)] in preindustrial (pre-1850) sediments specific to each core. For Hg, we modeled the
217 lithogenic and organic matter influences using linear regressions between Hg, Al, and sediment organic
218 matter in preindustrial sediment. The anthropogenic contribution to the concentration of Pb, Cd, or

Hg in sediment samples was estimated by re-arranging and solving Eq. 1 to obtain excess concentration.

Eq. 1 $$[Pb, Cd, Hg] = [lithogenic\ Pb, Cd, Hg] + [excess\ Pb, Cd, Hg]$$

Where $[Pb, Cd, Hg]$ is the concentration of Pb, Cd or Hg in a sediment sample, $[lithogenic\ Pb, Cd, Hg]$ is the predicted concentration of Pb, Cd or Hg from lithogenic metal contribution and organic matter accumulation (for Hg) that is estimated from Eq. 2 for Pb and Cd and from Eq. 3 for Hg.

Eq. 2 $$[lithogenic\ Pb, Cd] = \frac{[Pb,Cd]}{[Al]}_{(pre-1850)} \times [Al]$$

Where, $[lithogenic\ Pb, Cd]$ is the modeled lithogenic contribution to the concentration of Pb or Cd in a sediment sample, $\frac{[Pb,Cd]}{[Al]}_{(pre-1850)}$ is the ratio of Pb or Cd to Al in preindustrial sediment and $[Al]$ is the concentration of Al in the sediment sample. Ratios of Pb or Cd to Al in preindustrial sediment are available in the supplementary material (Supplementary Table S2).

Eq. 3 $$[modelled\ Hg] = a + b_{Al}[Al] + b_{OM}[OM]$$

Where *a* is the intercept of a multiple linear regression with the concentration of Al and organic matter as explanatory variables and Hg as a dependent variable in the preindustrial sediment. The variables b_{Al} and b_{OM} are the regression coefficients for the explanatory variables. Regressions were computed for each individual core, and therefore, the values for *a*, b_{Al} and b_{OM} varies by core. The values of the intercept, variable coefficients, coefficient of determination (R^2), and p-value for the multiple linear regression used for Eq. 3 are presented in the supplementary material in Table S3.

2.8 Geochemical fluxes calculation

The fluxes of each analyzed element, and including organic matter and carbonates (excluding charcoals), were calculated following equation 6.4:

Eq. 4 $$f_m = \frac{SR \times [m]}{FF}$$

Where f_m is the flux of a metal *m* (μg m^{-2} yr^{-1}), [m] is the metal *m* concentration (μg g^{-1}), SR is the modeled sedimentation rate (or mass accumulation rate) for the layer (g m^{-2} yr^{-1}) obtained from the CRS model, and FF is the sediment focusing factor (Blais and Kalff, 1995; Lehman, 1975), estimated as the ratio of regional atmospheric ^{210}Pb fallout to the observed unsupported ^{210}Pb flux at the sediment-water interface (Blais and Kalff, 1995; Muir et al., 2009; Wiklund et al., 2017). The local atmospheric ^{210}Pb deposition rate was estimated using the formula developed by Muir et al. (2009). In Eq. 4, [*m*] was substituted for the specific concentration predicted by lithogenic concentration, representative of catchment erosion (from Eq. 2 and 3) or anthropogenic excess (from solving Eq. 1) to obtain the corresponding component flux.

3. Results

3.1 Variation in sedimentation rates

Sedimentation rates were similar between sediment cores from the earliest modeled period (~1850) until the early 20th century (60 ± 35 g m^{-2} yr^{-1}), after which sedimentation rates doubled in Little Fox Lake and Fox Lake but remained relatively constant in Little Braeburn Lake and Grayling Lake (Figure 3).

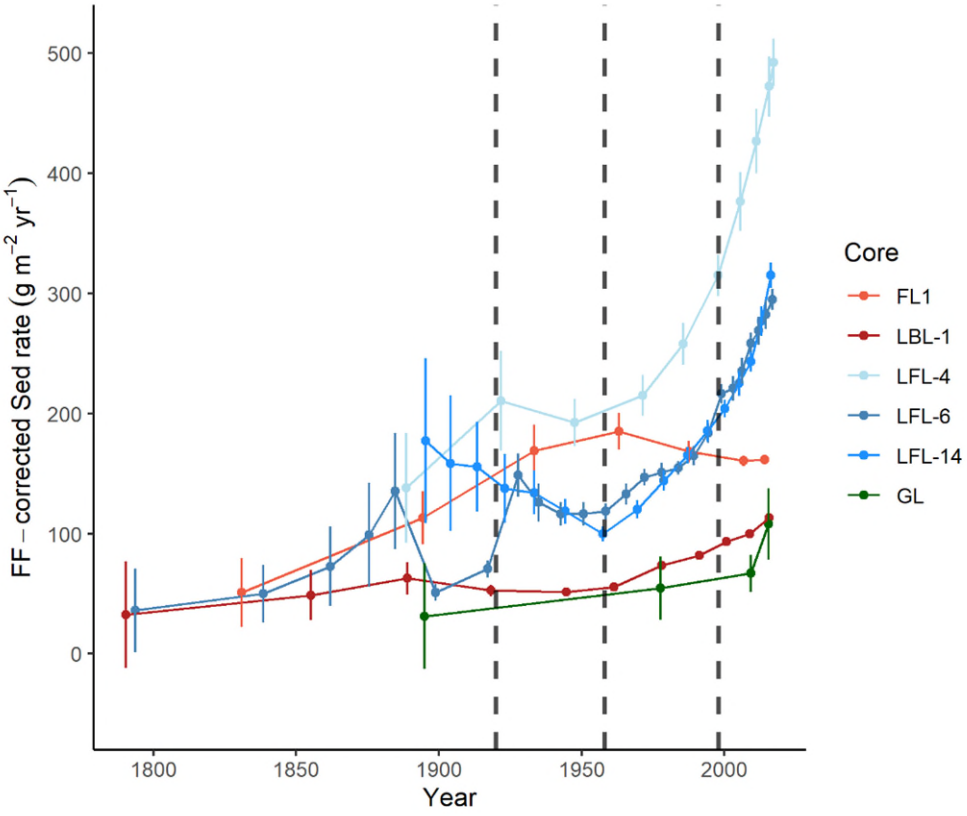

Figure 3: Modelled sedimentation rates (CRS model) and uncertainties against time in each core. The vertical dashed lines represent the occurrence of known wildfires events in the study area. The vertical error bars represent the flux uncertainty estimated by propagating the errors of the dating model.

The 1957-1958 wildfires triggered a slight increase in sedimentation rate at Little Braeburn Lake (Figure 3) that was primarily associated with a greater organic matter accumulation (Supplementary material, Figure S2). The same fire initiated an important increase in Little Fox Lake sedimentation rate (Figure 3), and the subsequent fire (in 1998) severely affected the Little Fox Lake catchment and caused further increase in this lake's sedimentation rate that persisted for the remainder of the sediment record (Figure 3). In contrast, the sedimentation rate in Little Braeburn Lake (unaffected by the 1998 wildfire) showed only a marginal change during the same period, and Fox Lake sedimentation rate slightly decreased over the same period (Figure 3). Compared to pre-1900 sediment layers, the

recent sedimentation rate is about two and three fold greater in Little Braeburn Lake and Fox Lake, respectively (120-175 g m^{-2} yr^{-1}) and five to eight fold greater (300-500 g m^{-2} yr^{-1}) in Little Fox Lake.

3.2 Fire exposure in each lake

The recorded charcoal accumulation rates (CHAR) in each lake sediment core generally agreed with the historical fire mapping of the area for all lakes but Little Braeburn Lake (Figure 4). However, the temporal resolution of the cores was limited by the slow sediment accumulation rate. Indeed, in sediment accumulated after 1950, a 1 cm interval corresponds to 5-25 years of sediment accumulation, depending on the core. This led to slight offset between know fire events and observed charcoal peaks in the sediment cores.

The CHAR magnitude was not directly proportional to the burned area in each lake catchment (supplementary material, Table S1). The magnitude of CHAR was 10-50 times greater in Little Fox Lake than in Fox Lake or Little Braeburn Lake. The small CHAR observed in Fox Lake (Figure 4a) was in agreement with the limited burned area in this lake's catchment indicated in the historical fire maps (Figure 1). In contrast, the small CHAR observed in the Little Braeburn Lake sediment record was surprising since historical fire maps suggested that all of the Little Braeburn Lake catchment burned between 1957 and 1958. The Little Braeburn Lake catchment was not burned during the 1998 fire, and yet, this fire event was recorded in the Little Braeburn Lake sediment as a peak in CHAR of similar magnitude to the 1957-1958 wildfire (Figure 4c). Therefore, Fox Lake and Little Braeburn Lake likely received primary charcoals from wildfire fallout during both the 1957-1958 and 1998 wildfires, but little to no charcoals from catchment surface erosion.

Little Fox Lake contrasts with Fox Lake and Little Braeburn Lake because the magnitude and aspect of peaks in CHAR indicated that charcoal particles were mostly transported by catchment erosion to Little Fox Lake in the years following the fire (Figure 4). Therefore, when using macroscopic charcoals

as a proxy for fire exposure, Little Fox Lake showed the greatest exposure to wildfires by far, followed by Little Braeburn Lake, where CHAR was low, but a large catchment surface was affected. Fox Lake serves as a control site with negligible fire impact. Grayling Lake showed slight increases in CHAR following the 1958 and 1998 wildfires that were of similar magnitude to Little Braeburn Lake (Figure 4b) and therefore suggest some primary charcoal transport in this lake as well, but CHAR magnitude in this lake is the smallest recorded. However, Grayling Lake sediment chronology has a very poor temporal resolution because of slow sediment accumulation rate and low ^{210}Pb activity in this core.

It should be noted that wildfire occurrence in Fox Lake, Little Fox Lake and Little Braeburn Lake was also evident from the charcoal concentration profiles and the charcoal area profiles, not just charcoal accumulation rates (Figure 5). One exception was observed in a core from Little Fox Lake (LFL-4), in which charcoal concentration increased with depth throughout the core and only one fire (1998) was evident from the variations in charcoal accumulaton rate (Figure 4e). With the exception of LFL-4, most cores are showing that variation in charcoal loading in lakes sediment was due to fire activity, not just caused by variation in sedimentation rates.

Interestingly, the charcoal accumulation history differed between the three cores from Little Fox Lake, which is likely related to the complex bathymetry of this lake (Supplementary information, Figure S4). While sediment from two sub-basins of the lake showed clear peaks from the 1998 fire (LFL-4 and LFL-14), the LFL-6 core showed a significant peak for the 1958 fire with a moderate peak for the 1998 fire (Figure 4). Differences in charcoal accumulation between different sections of the lake are likely representive of the proximity to burned slope and the gradient of these slopes, but historical fire mapping, especially for 1958 is not sufficiently accurate to explore this hypothesis in this study.

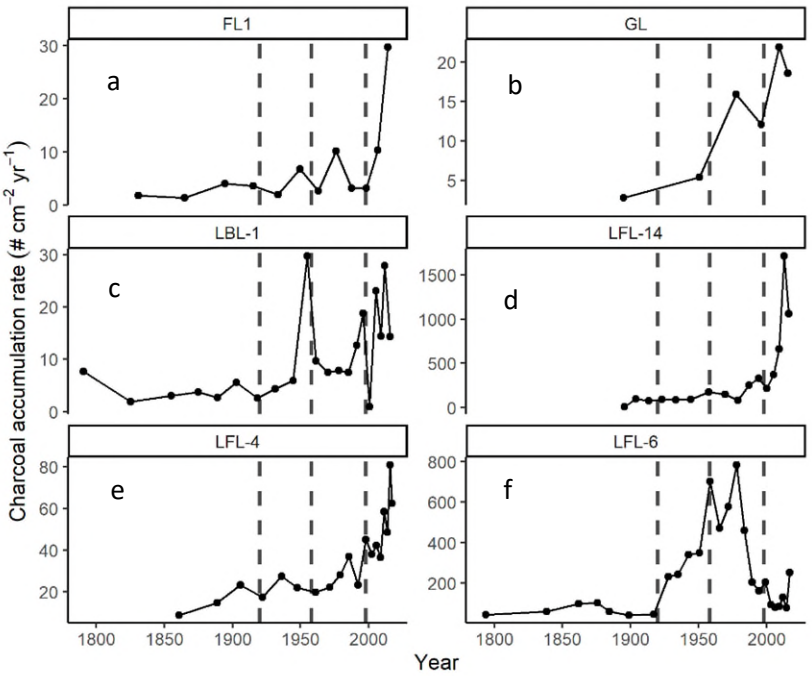

Figure 4: Focusing-factor-corrected charcoal accumulation rates in lake sediment cores of Fox Lake (FL1, a), Grayling Lake (GL, b), Little Braeburn Lake (LBL1, c), Little Fox Lake (LFL-14, d; LFL-4, e; LFL-6, f). The vertical dashed lines represent the years of major fires in the study area (1920, 1957-58, and 1998). Note the large difference in y-axis scales between lakes.

3.3 Concentrations of Hg, Pb, Cd, and indicator elements in lake sediment

Sediment metal concentrations varied both in the dated portion and undated bottom layers of each core (Figure 5). The concentration of Hg in the sediment of three study lakes increased by 40-100 ng g^{-1}, representing a 40-80% increase compared to baseline concentrations (Figure 5). The increasing Hg concentration in the top 10 cm of Little Braeburn Lake sediment was concurrent with increasing organic matter concentration (Figure 5). The correlation between organic matter and Hg concentration in the sediment of Little Braeburn Lake was strong and significant ($r=0.96$, $p<0.001$) whereas it was not significant in Fox Lake ($r=-0.16$, $p=0.35$) and weak in Grayling Lake ($r=0.43$, $p=0.002$). In the Little Fox Lake sediment the correlation between organic matter concentration and

Hg concentration was significant, yet weak, in two cores (LFL-6 and LFL-14, $r=0.49$-0.62, $p<0.001$) and insignificant in one core (LFL-4, $r= -0.06$, $p=0.62$). The important correlation between organic matter and Hg in Little Braeburn Lake suggest that greater organic matter accumulation and concentration may have driven changes in sediment Hg accumulation in this lake.

There was a clear sub-surface peak in Pb concentration in Fox Lake and Little Fox Lake (not Little Braeburn Lake), with Pb concentrations remaining 7-10 $\mu g\ g^{-1}$ above background values (75-120% increase) until the end of the record in 2018. The concentration of Cd increased by 0.2 $\mu g\ g^{-1}$ compared to background concentrations (20% increase) in Little Braeburn Lake and one core from Little Fox Lake (LFL-14) but remained stable or slightly decreased in Fox Lake and two other cores from Little Fox Lake (Figure 5).

The concentrations of Sr and Ca increased in the surface sediment of all lakes compared to older sediment, whereas the Ti concentration was following the opposite trend (Figure 5). Sediment phosphorus concentration increased in the larger lakes affected by wildfires (Little Fox Lake, Little Braeburn Lake) but not in Fox Lake and Grayling Lake.

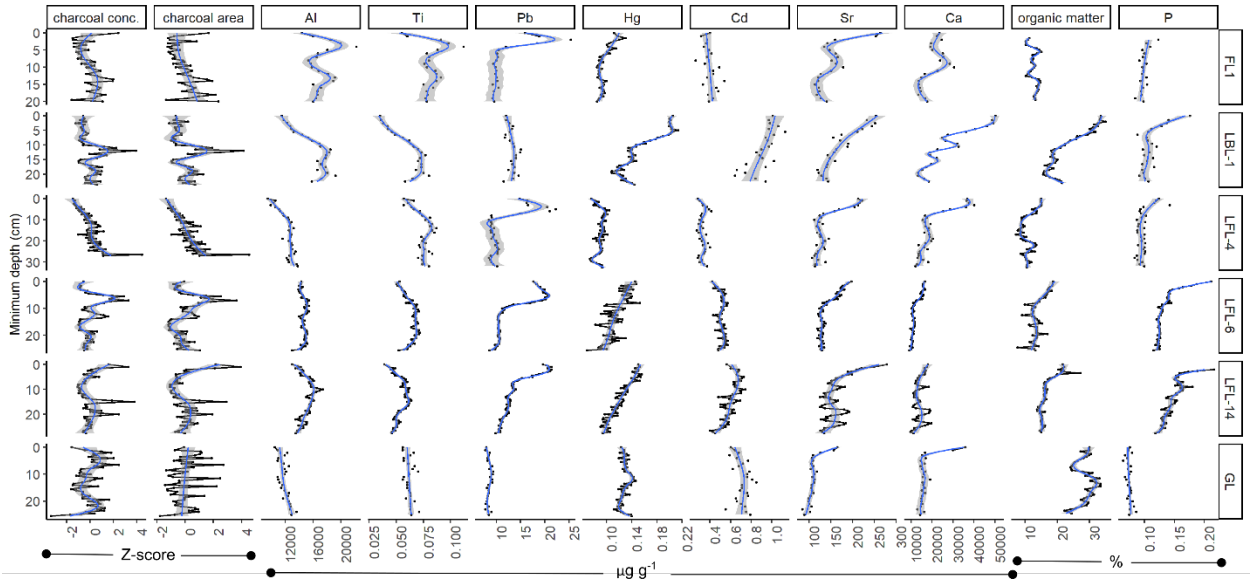

342

343 Figure 3: Element concentration profiles with depth in each Yukon lake sediment core with charcoal
344 concentration normalised (z-scored) by core. Blue lines are generalised additive models with a 95%
345 confidence interval (grey areas).

346 **3.4 Impact of wildfires on Hg, Pb, and Cd total and excess fluxes**

347 The fluxes of Hg, Pb, and Cd increased over time in the study lakes, especially over the last 60 years
348 (Figures 6, 7, and 8), both in response to higher sedimentation rate (Figure 3) and greater
349 concentrations of these elements in the sediment (Figure 5). The preindustrial (pre-1850) fluxes of Pb,
350 Hg, and Cd were small and comparable between all sites (Figures 6, 7, and 8). The 1958 wildfire was
351 concurrent with excess metal fluxes to the lakes of 11 ± 10 µg Hg m^{-2} yr^{-1} (maximum 29 µg Hg m^{-2} yr^{-1}),
352 1.8 ± 1.1 mg Pb m^{-2} yr^{-1} (maximum 2.9 mg Pb m^{-2} yr^{-1}), and 57 ± 66 µg Cd m^{-2} yr^{-1} (maximum 187
353 µg Cd m^{-2} yr^{-1}). The 1998 fire had a larger impact on metal fluxes, being concurrent with excess fluxes
354 of 25 ± 18 µg Hg m^{-2} yr^{-1} (maximum 58 µg Hg m^{-2} yr^{-1}), 3.2 ± 1.7 mg Pb m^{-2} yr^{-1} (maximum 4.7 mg Pb
355 m^{-2} yr^{-1}), and 107 ± 102 µg Cd m^{-2} yr^{-1} (maximum 306 µg Cd m^{-2} yr^{-1}).

The greatest increases in Hg, Pb, and Cd accumulation rates occurred in Little Fox Lake (Figures 6, 7, and 8). Those increases co-occurred with changes in charcoal accumulation rates, suggesting a link with the occurrence of wildfires. Unexpectedly, Little Fox Lake sedimentation rate and metal accumulation rates continued to increase over the twenty years that followed the 1998 fire instead of gradually returning towards the pre-fire accumulation rate. In contrast, Fox Lake (control site) had no visible increase in metal accumulation coinciding with wildfires (Figures 6, 7, and 8).

The accumulation rate of Pb in the most recent section of the records (2008-2018) was three to five times greater in Little Fox Lake (5-8 mg Pb m^{-2} yr^{-1}) than in Fox Lake (2-3 mg Pb m^{-2} yr^{-1}) and Little Braeburn Lake (1-2 mg Pb m^{-2} yr^{-1}). Similarly, the current Hg accumulation rate in Little Fox Lake (~40 µg Hg m^{-2} yr^{-1}) was twice the accumulation rate in Fox Lake and Little Braeburn Lake (~20 µg Hg m^{-2} yr^{-1}). The same was true for most metal elements, i.e., accumulation rates were 2-5 times greater in Little Fox Lake than Fox Lake and Little Braeburn Lake.

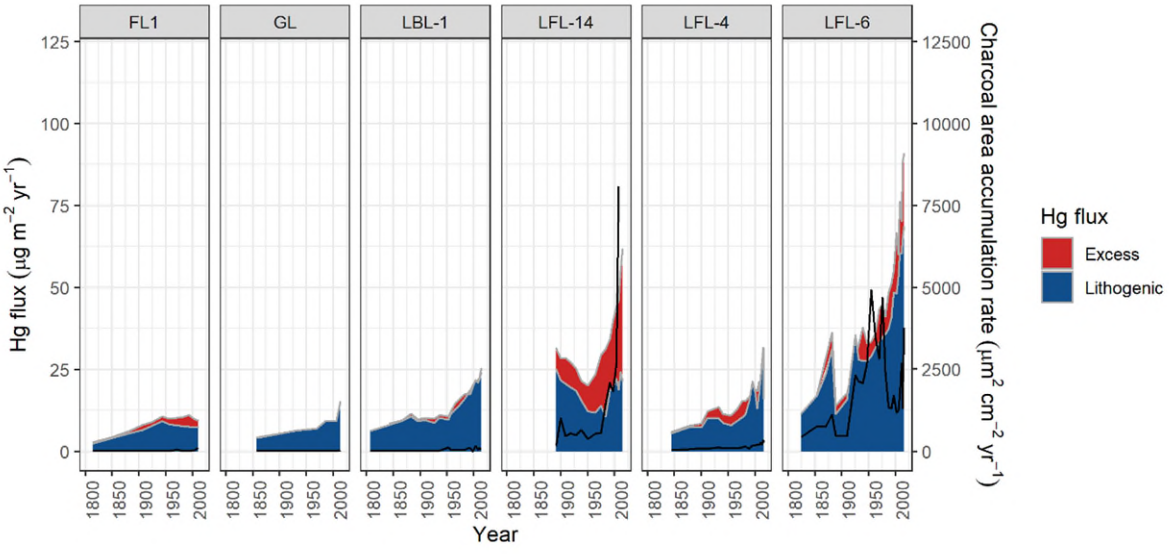

Figure 4: Deconstructed fluxes of Hg in each lake sediment following equations 6.1 and 6.3. The full black line represents the charcoal accumulation rate in each core and follows the secondary y-axis scale (right side).

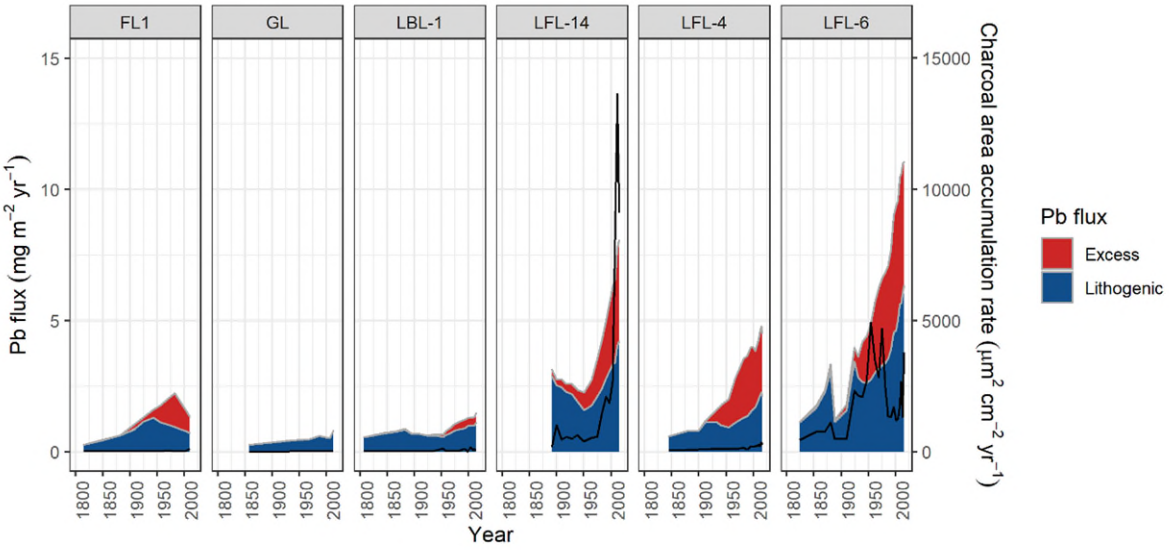

372

373 Figure 5: Deconstructed fluxes of Pb in each lake sediment following equations 6.1 and 6.2. The full
374 black line represents the charcoal accumulation rate in each core and follows the secondary y-axis scale
375 (right side).

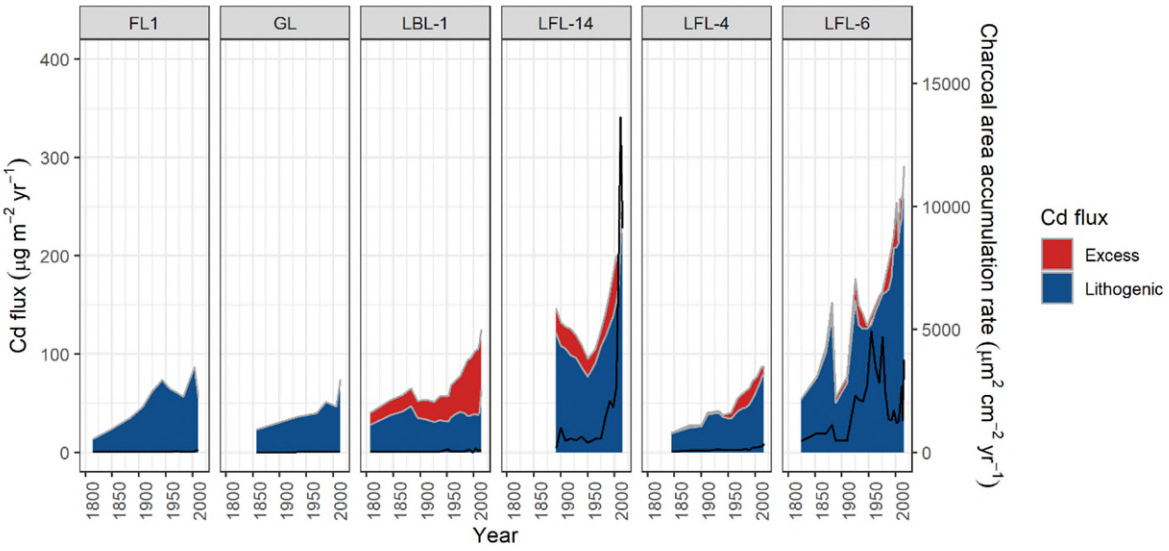

376

377 Figure 6: Deconstructed fluxes of Cd in each lake sediment following equations 6.1 and 6.2. The full
378 black line represents the charcoal accumulation rate in each core and follows the secondary y-axis scale
379 (right side).

Model estimates suggested that most variation in Hg, Pb, and Cd metal fluxes associated with wildfire events were caused by erosional (lithogenic) fluxes (Figures 6 to 8). Excess fluxes, i.e., those not predicted by changes in erosional fluxes or organic matter inputs (for Hg), contributed to a substantial proportion of the increase in the accumulation rate of Hg (Figure 6) and Pb (Figure 7) but were very small for Cd (Figure 8). Excess Hg fluxes increased in Fox Lake and Little Fox Lake but not in Little Braeburn Lake, where most of the increase in Hg accumulation was predictable from changes in organic matter accumulation (Figure 6). The excess Hg and Pb flux were similar in Fox Lake and Little Fox Lake until the 1958 wildfire, after which Hg fluxes increased faster in Little Fox lake than in Fox Lake (Figure 6), and Pb flux increased in Little Fox Lake, whereas it decreased in Fox Lake (Figure 7). Some excess fluxes of Cd are present after 1950 at all sites, but the fluxes were exceedingly small compared to natural inputs predicted from catchment erosion (Figure 8). Excess Cd was more important in Little Braeburn Lake than other lakes (Figure 8).

The cumulative impact of the two wildfires culminated in a four-to-six-fold increase in the accumulation rates of Ca, Ba, Sr, Ag, Hg, Se, and P in the Little Fox Lake sediment (Supplementary information, Figure S3) and the concentrations of these elements in the sediment were greater post-wildfires (Supplementary information, Figure S5). Furthermore, the accumulation rates of every other analyzed element were also two to four times greater during the two decades that followed the 1998 wildfire.

4. Discussion

4.1 Importance of wildfires for the terrestrial transport of metals to subarctic mountane lakes

The large increase in sedimentation rate (2-5 fold) and Hg, Pb, and Cd loading (4-6 fold) in the sediment of Little Fox Lake occurring after the two wildfires in 1958 and 1998 showed that wildfires

403 can strongly impact the loading of these elements in subarctic lakes. When comparing the sediment
404 accumulation history of all four study lakes, we found the largest increase in Hg, Pb and Cd
405 accumulation by far in the lake that was most impacted by wildfires in recent decades (Little Fox Lake).
406 This wildfire influence was evident from historical fire maps and charcoal accumulation history in the
407 lake, where sediment charcoal accumulation rates and concentrations were 10-100 times greater in
408 Little Fox Lake than any other lake (Figures 5 and 6). The Hg and Pb accumulation rates in Little Fox
409 Lake in recent decades surpassed the accumulation rate recorded for the periods with the largest
410 anthropogenic emissions of theses contaminants, whereas these periods are easily identifiable in
411 sediment from lakes unaffected by those fires, such as Fox Lake in this study (Figures 6, 7 and 8). This
412 shows that in the future, wildfires may modulate the response of northern lakes to varying atmospheric
413 deposition of Pb and Hg.

414 More stable sedimentation and metal accumulation rates in Fox Lake and Little Braeburn Lake, largely
415 unexposed to the 1998 wildfire, indicated that the critical changes observed in Little Fox Lake
416 sediments were not due to regional pollution, road construction, or any other factor than the fires.
417 This study showed that in burned catchments, the effect of erosional processes on lake metal loading
418 can be orders of magnitude higher than metal loading caused solely by atmospheric deposition of ash
419 during the fire (Pelletier et al., 2020).

420 In the years that followed the 1998 fire, Hg fluxes recorded in Little Fox Lake sediment were 2.5 to 5
421 times greater than values reported in two nearby lakes of the same ecoregion where wildfires were
422 absent. The total excess flux of Hg derived from Little Fox Lake's burned catchment (~12-50 μg m^{-2}
423 yr^{-1}) represents a comparable or larger excess Hg flux than in the industrialized Athabasca Oil Sand
424 Region (11.4 ± 7.8 μg m−2 yr−1, Roberts et al., 2021) and 5-10% of the excess Hg flux observed in
425 lakes around the Flin-Flon metal smelter in Manitoba (436 ± 614 μg m−2 yr−1, Roberts et al., 2021).

426 The excess Hg flux in Little Fox Lake represents 4 to 16 times the direct annual atmospheric Hg flux
427 to Kusawa Lake (Zdanowicz et al., 2018), which is located about 180 km away from Little Fox Lake.
428 The concentration of Hg in Little Fox Lake sediment was also 1.6 to 2 times greater than sediment of
429 equivalent age at Kluane Lake, which is located 200 km away and did not experience important
430 wildfires over that period (Zabel et al., 2021). The average atmospheric Pb flux in southwestern
431 Yukon, estimated with ice cores (Gross et al., 2012), was < 1 mg m^{-2} yr^{-}, which is far less than the 2.7
432 - 4.7 mg Pb m^{-2} yr^{-1} increase in Pb flux associated with wildfires in Little Fox Lake. These comparisons
433 highlight the importance of wildlfire-driven Hg and Pb fluxes to lakes in the region.

434 Milder impacts were observed from the 1958 fire in Little Braeburn Lake (which remained untouched
435 by the 1998 fire) than in the 1958 or 1998 fires around Little Fox Lake. Despite the smaller changes
436 in sedimentation rate in Little Braeburn Lake compared to Little Fox Lake, the concentration of
437 organic matter, Sr, and Ca in the Little Braeburn Lake sediment increased continuously after the fire,
438 indicating greater rates of catchment weatheringand larger input of catchment-derived material to the
439 lake (Dasch, 1969; Probst et al., 2000; Xu et al., 2010). The impact of catchment erosion caused by
440 the wildfire around Little Braeburn Lake had a moderate impact on Hg and Cd accumulation in the
441 sediment (Figures 6 and 8), but no impact on Pb accumulation (Figure 7). Increased sediment organic
442 matter in Little Braeburn Lake sediment may have been related to increased lake production from
443 nutrients released by the fire and transported in surface and groundwater flow through time
444 (Pompeani et al., 2020; Rhoades et al., 2019). Other long sediment records have shown that increases
445 in lake nutrient input have been shown to persist for 20-30 years following fires in the lake catchment
446 (Dunnette et al., 2014; Pompeani et al., 2020). Alternatively, since an important layer of soil organic
447 matter was preserved in Little Braeburn Lake (Figure 2), loading of organic matter to Little Braeburn
448 Lake post-1958 may have been primarily from catchment erosion.

4.2 Influences of slopes and lake bathymetry on wildfire effects

The important impact of wildfires on erosion rate and lake metal loading observed in this study were likely modulated by the slope gradient near the study lakes. Little Fox Lake is surrounded by steeper slopes (23-32% gradient) that end closer to the lake shore compared to Little Braeburn Lake (7-12% gradient) and Grayling Lake (surrounded by flat wetland) (Figure 1). The evidence that slopes are playing an important role in transporting Hg, Pb, and Cd to lakes include the low impact on sedimentation rate and metal concentrations observed in Grayling Lake despite this lake being included within the 1998 fire scar. Similarly, Little Braeburn Lake was included within the 1957-1958 wildfire zone but showed relatively low changes in sedimentation rates following this fire compared with Little Fox Lake (Figures 3, 4, 5 and 6). Burned catchments with steeper slopes erode faster because unsaturated flow is accelerated (Ebel, 2013) and surface flows peak more heavily during storm events (Ice et al., 2004; Shakesby, 2011). In contrast, lower slope gradients may limit wildfire-driven erosion by allowing more organic soil to build up in low-relief areas capable of retaining water, sediments, and leachates (Johnston, 1991). Future efforts to predict the fate of legacy anthropogenic metals such as Pb and Hg accumulated on the subarctic landscape will therefore need to carefully consider the slope transport processes around lakes as an essential predictor of impact on lakes.

Little Fox Lake has a complex bathymetry composed of multiple sub-basins (Supplementary material, Figure S4), hence the need to use multiple cores to assess fire impacts. Interestingly, we observed a different pattern of charcoal accumulation in the different sub-basins of this lake and the differences were likely due different sediment transport processed linked to the proximity of the sub-basin to the burned catchment during each fire event. Cores from the West or East basin of the lake recorded the fires occurring in the corresponding catchment section (Figure 4). The changes in metal(loid)

accumulation caused by the wildfire also varied throughout the lake and led to different metal(loid) accumulation rates, especially for Hg and Cd (Figures 6 and 8). The basin where the LFL-4 core was collected had lower inputs of charcoal and lower metal accumulation compared to the other two sub-basins. The complex bathymetry of Little Fox Lake and the different charcoal accumulation history in the three cores suggest that each sub-basin of the lakes receives sediment from a slightly different section of the catchment, which may not have been equally affected by the wildfires and may have different soil composition.

4.3 Transport of anthropogenic metals by wildfires

A substantial portion of the Hg and Pb accumulated in the sediment of Little Fox Lake exceeded amounts predicted by elemental ratios with Al in preindustrial sediment (Figures 6 and 7). This excess is commonly attributed to anthropogenic pollution in paleolimnological studies using similar approaches (e.g., Furl and Meredith, 2011; Perry et al., 2005; Pelletier et al., 2021). In lakes that were least exposed to the wildfires, the accumulation rate of excess Hg and Pb is consistent with other studies reporting a slow increase in Hg and Pb deposition in northwestern Canada starting around the Industrial Revolution (~1850), accelerating in the mid-20th century (~1945) and decreasing after 1970 for Pb (Bindler, 2011; Marx et al., 2016) or for Hg, reaching a plateau around the same time (Cooke et al., 2020; Drevnick et al., 2012; Korosi et al., 2018). However, wildfires promoted greater fluxes and concentrations of Pb and Hg (of possible anthropogenic origin) in Little Fox Lake. The timing of these fluxes were inconsistent with known historical emissions of these contaminants to the atmosphere. Greater rates of excess (anthropogenic) Pb and Hg accumulation in Little Fox Lake than in other study lakes and the discrepancy between the expected peak periods of accumulation of these elements and those observed peak periods in the sediment records indicate that wildfires may have played a role in transporting legacy anthropogenic Pb and Hg to the lake. The last 60 years of sediment

accumulation in Little Fox Lake demonstrates that wildfires can impede the recovery from anthropogenic Pb and Hg pollution in mountainous subarctic watersheds, even when the atmospheric deposition rate of these elements declines or remains stable (Pelletier et al., 2021; Shotyk et al., 2016). It is important to note that our estimation of lithogenic Hg, Pb and Cd fluxes are based on pre-industrial ratios of these elements to Al and therefore, concurrent Al inputs from a source other than burned soils would lead to underestimation of anthropogenic (excess) fluxes. Stable isotopes of Pb and Hg would provide more definitive tracers to distinguish local lithogenic sources from long-range anthropogenic sources of those metals as well changes in source contributions to the lake sediments over time (Odigie and Flegal, 2011; Tsui et al., 2020).

4.4 Recovery (or lack of recovery) from wildfires

In long-term lake sediment reconstructions, the typical geochemical impact of wildfires in Colorado alpine lakes typically lasted for 20-30 years following fire events during the Holocene (Dunnette et al., 2014; Leys et al., 2016; Pompeani et al., 2020). In contrast, the impact of the 1998 fire in Little Fox Lake was ongoing and gaining in magnitude 20 years after the fire event. The surprising extent of the impact is likely related to the poor vegetation recovery and the near absence of soil organic matter in the lake's catchment (Figure 2). Severe or frequent wildfires can impede normal vegetation recovery past a certain threshold (McLauchlan et al., 2020; Stevens-Rumann and Morgan, 2019) and such thresholds are frequently surpassed in similar subalpine and subarctic ecosystems such as Wyoming subalpine lodgepole pine forests (Turner et al., 2019) and Yukon subarctic black spruce forests (Brown and Johnstone, 2012). In Little Fox Lake, the rapid return interval between wildfires (40 years) and the minor vegetation recovery observed 20 years after the wildfire suggests a fire severity threshold may have been exceeded, leading to slow ecosystem recovery. Because climate change is increasing the frequency and the severity of subarctic and boreal wildfires (Chen et al., 2021; Kelly et al., 2013;

518 Sae-Lim et al., 2019), situations like Little Fox Lake may become more common in the near future,
519 and wildfires may play a greater role in the accumulation and concentrations of Hg, Pb, and Cd in lake
520 sediment.

521 **5. Conclusion**

522 This study showed impacts of wildfires on the accumulation of Hg, Pb and Cd in sediment of subarctic
523 montane lakes. We observed mild impacts of wildfires on sedimentation rate, organic matter, and
524 loading of Hg, Pb, and Cd where fire exposure was minor (Fox Lake, Little Braeburn Lake, and
525 Grayling Lake), but severe impacts where catchment fire exposure was more important and vegetation
526 recovery was limited (Little Fox Lake). Large changes in catchment erosion followed the two severe
527 wildfires in Little Fox Lake. Erosion accelerated the transport of Hg, Pb, and Cd from the catchment
528 to the lake, in contrast with effects to other lakes of the same valley less exposed to wildfires.

529 Since subarctic wildfire frequency and intensity are predicted to increase in the following decades,
530 greater release from wildfires of Hg, Pb, Cd in mountane lakes and streams could have implications
531 for surface water quality and for future exposure of biota to these elements. In areas where
532 atmospheric deposition of these elements has declined in response to recent regulations of
533 anthropogenic emissions, more intense or more frequent wildfires could delay the recovery of aquatic
534 ecosystems toward preindustrial levels of contaminants.

535 Future monitoring and paleoenvironmental studies should evaluate the impact of wildfires on the
536 release of legacy contaminants in different geophysical regions and in areas where multiple climatic
537 pressures may intersect. For example, areas affected by precipitation changes, permafrost thaw, and
538 wildfires simultaneously may experience the most rapid release of legacy contaminants to aquatic
539 ecosystems. The factors influencing future loadings of Pb, Hg, and Cd to subarctic lakes include the
540 total inventory of anthropogenic contaminants in subarctic soils, their distribution in soil profiles,

future catchment erosion rates, and future wildfire activity. Recent mapping of anthropogenic Hg in soils has been conducted in Alaska, and a similar investigation in the Canadian subarctic and for different contaminants (e.g., Hg, Pb, Cd) would be beneficial to evaluate the vulnerability of legacy metals to be remobilized to surface waters.

Credit authorship contribution statement

Nicolas Pelletier: Conceptualization, Investigation, Formal analysis, Writing – original draft, Writing – review and editing. **John Chételat:** Conceptualization, Writing – review and editing, Supervision, Funding acquisition. **Sarah Sinon:** Investigation, Formal analysis. **Jesse C. Vermaire:** Conceptualization, Investigation, Writing – review and editing, Supervision, Funding acquisition.

Appendix A: Supplementary Data

Supplementary data to this article can be found online at https:\\doi.

Acknowledgements

The project was realized with permission from the Ta'an Kwach'an Council and the Yukon Tourism and Culture Board. Thank you to Alexandra Steffen for help with initiating the research and site interpretation, to Michael J. Murphy for assistance with fieldwork, and to Brian Horton for sample storage. Thank you to Christine McClelland for assistance with sample processing in the laboratory.

Funding

This research was supported with funding from Environment and Climate Change Canada and Natural Sciences and Engineering Research Council (NSERC) Discovery Grants to JC (06159-2016) and JCV (05257-2015). Nicolas Pelletier was funded by the Fonds de Recherche du Québec - Nature et technologies, Ontario Graduate Scholarship, the Northern Student Training Program, and Environment and Climate Change Canada.

Declaration of Competing Interests

The authors declare that they have no known competing financial interests or personal relationships that could have appeared to influence the work reported in this paper.

566 **References**

567 Abbate, Longoni, Ivanov, and Papini. (2019). Wildfire Impacts on Slope Stability Triggering in
568 Mountain Areas. *Geosciences*, *9*(10), 417. https://doi.org/10.3390/geosciences9100417

569 Abraham, J., Dowling, K., and Florentine, S. (2017). Risk of post-fire metal mobilization into surface
570 water resources: A review. *Science of The Total Environment*, *599–600*, 1740–1755.
571 https://doi.org/10.1016/j.scitotenv.2017.05.096

572 Abraham, J., Dowling, K., and Florentine, S. (2018). Controlled burn and immediate mobilization of
573 potentially toxic elements in soil, from a legacy mine site in Central Victoria, Australia. *Science of*
574 *The Total Environment*, *616–617*, 1022–1034.
575 https://doi.org/10.1016/J.SCITOTENV.2017.10.216

576 Appleby, P. G., and Oldfield, F. (1978). The calculation of lead-210 dates assuming a constant rate
577 of supply of unsupported 210Pb to the sediment. *CATENA*, *5*(1), 1–8.
578 https://doi.org/10.1016/S0341-8162(78)80002-2

579 Bao, K., Shen, J., Wang, G., and Roux, G. (2015). Atmospheric Deposition History of Trace Metals
580 and Metalloids for the Last 200 Years Recorded by Three Peat Cores in Great Hinggan
581 Mountain, Northeast China. *Atmosphere*, *6*(3), 380–409. https://doi.org/10.3390/atmos6030380

582 Bindler, R. (2011). Contaminated lead environments of man: reviewing the lead isotopic evidence in
583 sediments, peat, and soils for the temporal and spatial patterns of atmospheric lead pollution in
584 Sweden. *Environmental Geochemistry and Health*, *33*(4), 311–329. https://doi.org/10.1007/s10653-
585 011-9381-7

586 Blais, J., and Kalff, J. (1995). The influence of lake morphometry on sediment focusing. *Limnology*
587 *and Oceanography*, *40*(3), 582–588. https://doi.org/10.4319/lo.1995.40.3.0582

588 Bodí, M. B., Martin, D. A., Balfour, V. N., Santín, C., Doerr, S. H., Pereira, P., et al. (2014). Wildland
589 fire ash: Production, composition and eco-hydro-geomorphic effects. *Earth-Science Reviews*, *130*,

590 103–127. https://doi.org/10.1016/j.earscirev.2013.12.007
591 Brown, C. D., and Johnstone, J. F. (2012). Once burned, twice shy: Repeat fires reduce seed
592 availability and alter substrate constraints on Picea mariana regeneration. *Forest Ecology and*
593 *Management*, *266*, 34–41. https://doi.org/10.1016/j.foreco.2011.11.006
594 Burton, C. A., Hoefen, T. M., Plumlee, G. S., Baumberger, K. L., Backlin, A. R., Gallegos, E., and
595 Fisher, R. N. (2016). Trace Elements in Stormflow, Ash, and Burned Soil following the 2009
596 Station Fire in Southern California. *PloS One*, *11*(5), e0153372.
597 https://doi.org/10.1371/journal.pone.0153372
598 Campos, I., Vale, C., Abrantes, N., Keizer, J. J., and Pereira, P. (2015). Effects of wildfire on
599 mercury mobilisation in eucalypt and pine forests. *CATENA*, *131*, 149–159.
600 https://doi.org/10.1016/j.catena.2015.02.024
601 Cerrato, J. M., Blake, J. M., Hirani, C., Clark, A. L., Ali, A.-M. S., Artyushkova, K., et al. (2016).
602 Wildfires and water chemistry: effect of metals associated with wood ash. *Environmental Science-*
603 *Processes and Impacts*, *18*(8), 1078–1089. https://doi.org/10.1039/c6em00123h
604 Chen, Y., Romps, D. M., Seeley, J. T., Veraverbeke, S., Riley, W. J., Mekonnen, Z. A., and
605 Randerson, J. T. (2021). Future increases in Arctic lightning and fire risk for permafrost carbon.
606 *Nature Climate Change 2021 11:5*, *11*(5), 404–410. https://doi.org/10.1038/s41558-021-01011-y
607 Coogan, S. C. P., Robinne, F.-N., Jain, P., and Flannigan, M. D. (2019). Scientists' warning on
608 wildfire — a Canadian perspective. *Canadian Journal of Forest Research*, *49*(9), 1015–1023.
609 https://doi.org/10.1139/cjfr-2019-0094
610 Cooke, C. A., Martínez-Cortizas, A., Bindler, R., and Sexauer Gustin, M. (2020). Environmental
611 archives of atmospheric Hg deposition – A review. *Science of the Total Environment*, *709*, 134800.
612 https://doi.org/10.1016/j.scitotenv.2019.134800
613 Dasch, E. J. (1969). Strontium isotopes in weathering profiles, deep-sea sediments, and sedimentary

614 rocks. *Geochimica et Cosmochimica Acta*, *33*(12), 1521–1552. https://doi.org/10.1016/0016-
615 7037(69)90153-7
616 Dijkstra, J. A., Buckman, K. L., Ward, D., Evans, D. W., Dionne, M., and Chen, C. Y. (2013).
617 Experimental and Natural Warming Elevates Mercury Concentrations in Estuarine Fish. *PLoS*
618 *ONE*, *8*(3), e58401. https://doi.org/10.1371/journal.pone.0058401
619 Drevnick, P. E., Engstrom, D. R., Driscoll, C. T., Swain, E. B., Balogh, S. J., Kamman, N. C., et al.
620 (2012). Spatial and temporal patterns of mercury accumulation in lacustrine sediments across
621 the Laurentian Great Lakes region. *Environmental Pollution*, *161*, 252–260.
622 https://doi.org/10.1016/j.envpol.2011.05.025
623 Dunnette, P. V, Higuera, P. E., McLauchlan, K. K., Derr, K. M., Briles, C. E., and Keefe, M. H.
624 (2014). Biogeochemical impacts of wildfires over four millennia in a Rocky Mountain subalpine
625 watershed. *New Phytologist*, *203*(3), 900–912. https://doi.org/10.1111/nph.12828
626 Ebel, B. A. (2013). Simulated unsaturated flow processes after wildfire and interactions with slope
627 aspect. *Water Resources Research*, *49*(12), 8090–8107. https://doi.org/10.1002/2013WR014129
628 ECCC. (2010). Canadian Climate Normals, 1981–2010 Whitehorse station data, Ottawa, Canada:
629 Environment and Climate ChangeCanada. https://climate.weather.gc.ca/climate_normals/
630 Evans, C. D., Malcolm, I. A., Shilland, E. M., Rose, N. L., Turner, S. D., Crilly, A., et al. (2017).
631 Sustained Biogeochemical Impacts of Wildfire in a Mountain Lake Catchment. *Ecosystems*,
632 *20*(4), 813–829. https://doi.org/10.1007/s10021-016-0064-1
633 Feyte, S., Tessier, A., Gobeil, C., and Cossa, D. (2010). In situ adsorption of mercury,
634 methylmercury and other elements by iron oxyhydroxides and organic matter in lake sediments.
635 *Applied Geochemistry*, *25*(7), 984–995. https://doi.org/10.1016/j.apgeochem.2010.04.005
636 Feyte, S., Gobeil, C., Tessier, A., and Cossa, D. (2012). Mercury dynamics in lake sediments.
637 *Geochimica et Cosmochimica Acta*, *82*, 92–112. https://doi.org/10.1016/j.gca.2011.02.007

638 Filgueira, C. F., and Vega, J. A. (2006). Runoff and soil erosion after rainfall simulations in burned
639 soils Development of the Forest Fire Danger Forecast System of Mexico View project
640 GEPRIF (geprif.agripa.org) View project. *Article in Forest Ecology and Management*.
641 https://doi.org/10.1016/j.foreco.2006.08.310
642 Furl, C. V., and Meredith, C. A. (2011). Mercury accumulation in sediment cores from three
643 Washington state lakes: Evidence for local deposition from a coal-fired power plant. *Archives of*
644 *Environmental Contamination and Toxicology*, *60*(1), 26–33. https://doi.org/10.1007/s00244-010-
645 9530-5
646 Garcia, E., and Carignan, R. (2005). Mercury concentrations in fish from forest harvesting and fire-
647 impacted Canadian Boreal lakes compared using stable isotopes of nitrogen. *Environmental*
648 *Toxicology and Chemistry*, *24*(3), 685–693. https://doi.org/10.1897/04-065R.1
649 Garcia, E., Carignan, R., and Lean, D. R. S. (2007). Seasonal and inter-annual variations in methyl
650 mercury concentrations in zooplankton from boreal lakes impacted by deforestation or natural
651 forest fires. *Environmental Monitoring and Assessment*, *131*(1–3), 1–11.
652 https://doi.org/10.1007/s10661-006-9442-z
653 Harper, A. R., Santin, C., Doerr, S. H., Froyd, C. A., Albini, D., Otero, X. L., et al. (2019). Chemical
654 composition of wildfire ash produced in contrasting ecosystems and its toxicity to Daphnia
655 magna. *International Journal of Wildland Fire*, *28*(10), 726. https://doi.org/10.1071/WF18200
656 Ice, G. G., Neary, D. G., and Adams, P. W. (2004). Effects of Wildfire on Soils and Watershed
657 Processes. *Journal of Forestry*, *102*(6), 16–20.
658 Isley, C. F., and Taylor, M. P. (2020). Atmospheric remobilization of natural and anthropogenic
659 contaminants during wildfires. *Environmental Pollution*, *267*, 115400.
660 https://doi.org/10.1016/j.envpol.2020.115400
661 Jensen, A. M., Scanlon, T. M., and Riscassi, A. L. (2017). Emerging investigator series: the effect of

wildfire on streamwater mercury and organic carbon in a forested watershed in the southeastern United States. *Environmental Science: Processes and Impacts*, *19*(12), 1505–1517. https://doi.org/10.1039/C7EM00419B

Johnston, C. A. (1991). Sediment and nutrient retention by freshwater wetlands: Effects on surface water quality. *Critical Reviews in Environmental Control*, *21*(5–6), 491–565. https://doi.org/10.1080/10643389109388425

Kelly, E. N., Schindler, D. W., Louis, V. L. S., Donald, D. B., and Vladicka, K. E. (2006). Forest fire increases mercury accumulation by fishes via food web restructuring and increased mercury inputs. *Proceedings of the National Academy of Sciences*, *103*(51), 19380–19385. https://doi.org/10.1073/pnas.0609798104

Kelly, R., Chipman, M. L., Higuera, P. E., Stefanova, I., Brubaker, L. B., and Hu, F. S. (2013). Recent burning of boreal forests exceeds fire regime limits of the past 10,000 years. *Proceedings of the National Academy of Sciences*, *110*(32), 13055–13060. https://doi.org/10.1073/PNAS.1305069110

Kitzberger, T., Falk, D. A., Westerling, A. L., and Swetnam, T. W. (2017). Direct and indirect climate controls predict heterogeneous early-mid 21st century wildfire burned area across western and boreal North America. *PLOS ONE*, *12*(12), e0188486. https://doi.org/10.1371/journal.pone.0188486

Kohlenberg, A. J., Turetsky, M. R., Thompson, D. K., Branfireun, B. A., and Mitchell, C. P. J. (2018). Controls on boreal peat combustion and resulting emissions of carbon and mercury. *Environmental Research Letters*, *13*(3), 35005. https://doi.org/10.1088/1748-9326/aa9ea8

Korosi, J. B., Griffiths, K., Smol, J. P., and Blais, J. M. (2018). Trends in historical mercury deposition inferred from lake sediment cores across a climate gradient in the Canadian High Arctic. *Environmental Pollution*, *241*, 459–467. https://doi.org/10.1016/j.envpol.2018.05.049

686 Krawchuk, M. A., Moritz, M. A., Parisien, M.-A., Van Dorn, J., and Hayhoe, K. (2009). Global
687 Pyrogeography: the Current and Future Distribution of Wildfire. *PLoS ONE*, *4*(4), e5102.
688 https://doi.org/10.1371/journal.pone.0005102
689 Lehman, J. T. (1975). Reconstructing the rate of accumulation of lake sediment: The effect of
690 sediment focusing. *Quaternary Research*, *5*(4), 541–550. https://doi.org/10.1016/0033-
691 5894(75)90015-0
692 Leys, B., Higuera, P. E., McLauchlan, K. K., and Dunnette, P. V. (2016). Wildfires and geochemical
693 change in a subalpine forest over the past six millennia. *Environmental Research Letters*, *11*(12),
694 125003. https://doi.org/10.1088/1748-9326/11/12/125003
695 Marcantonio, R. (2007). *A 1200-year record of forest fire history from macroscopic charcoal preserved in lake*
696 *sediment, south-central Yukon Territory*. Carleton University.
697 https://doi.org/https://doi.org/10.22215/etd/2007-07664
698 Marx, S. K., Rashid, S., and Stromsoe, N. (2016, June 1). Global-scale patterns in anthropogenic Pb
699 contamination reconstructed from natural archives. *Environmental Pollution*. Elsevier Ltd.
700 https://doi.org/10.1016/j.envpol.2016.02.006
701 McLauchlan, K. K., Higuera, P. E., Miesel, J., Rogers, B. M., Schweitzer, J., Shuman, J. K., et al.
702 (2020, September 1). Fire as a fundamental ecological process: Research advances and frontiers.
703 *Journal of Ecology*. Blackwell Publishing Ltd. https://doi.org/10.1111/1365-2745.13403
704 Meng, R., Dennison, P. E., Huang, C., Moritz, M. A., and D'Antonio, C. (2015). Effects of fire
705 severity and post-fire climate on short-term vegetation recovery of mixed-conifer and red fir
706 forests in the Sierra Nevada Mountains of California. *Remote Sensing of Environment*, *171*, 311–
707 325. https://doi.org/10.1016/j.rse.2015.10.024
708 Muir, D. C. G., Wang, X., Yang, F., Nguyen, N., Jackson, T. A., Evans, M. S., et al. (2009). Spatial
709 Trends and Historical Deposition of Mercury in Eastern and Northern Canada Inferred from

Lake Sediment Cores. *Environmental Science and Technology*, *43*(13), 4802–4809. https://doi.org/10.1021/es8035412

Nzihou, A., and Stanmore, B. (2013, July 5). The fate of heavy metals during combustion and gasification of contaminated biomass-A brief review. *Journal of Hazardous Materials*. Elsevier. https://doi.org/10.1016/j.jhazmat.2013.02.050

Odigie, K. O., and Flegal, A. R. (2011). Pyrogenic Remobilization of Historic Industrial Lead Depositions. *Environmental Science and Technology*, *45*(15), 6290–6295. https://doi.org/10.1021/es200944w

Odigie, K. O., and Flegal, A. R. (2014). Trace Metal Inventories and Lead Isotopic Composition Chronicle a Forest Fire's Remobilization of Industrial Contaminants Deposited in the Angeles National Forest. *PLOS ONE*, *9*(9), e107835. https://doi.org/10.1371/journal.pone.0107835

Odigie, K. O., Khanis, E., Hibdon, S. A., Jana, P., Araneda, A., Urrutia, R., and Flegal, A. R. (2015). Remobilization of trace elements by forest fire in Patagonia, Chile. *Regional Environmental Change*, *16*(4), 1089–1096. https://doi.org/10.1007/s10113-015-0825-y

Paterson, A. M., Morimoto, D. S., Cumming, B. F., Smol, J. P., and Szeicz, J. M. (2002). A paleolimnological investigation of the effects of forest fire on lake water quality in northwestern Ontario over the past ca. 150 years. *Canadian Journal of Botany*, *80*(12), 1329–1336. https://doi.org/10.1139/b02-117

Pelletier, N., Chételat, J., Blarquez, O., and Vermaire, J. C. (2020). Paleolimnological assessment of wildfire-derived atmospheric deposition of trace metal (loid)s and major ions to subarctic lakes (Northwest Territories, Canada). *Journal of Geophysical Research: Biogeosciences*. https://doi.org/10.1029/2020jg005720

Pelletier, N., Chételat, J., Palmer, M. J., and Vermaire, J. C. (2021). Bog and lake sediment archives reveal a lagged response of subarctic lakes to diminishing atmospheric Hg and Pb deposition.

734 *Science of The Total Environment*, 145521. https://doi.org/10.1016/j.scitotenv.2021.145521
735 Pereira, P., and Úbeda, X. (2010). Spatial distribution of heavy metals released from ashes after a
736 wildfire. *Journal of Environmental Engineering and Landscape Management*, *18*(1), 13–22.
737 https://doi.org/10.3846/jeelm.2010.02
738 Perry, E., Norton, S. A., Kamman, N. C., Lorey, P. M., and Driscoll, C. T. (2005). Deconstruction of
739 historic mercury accumulation in lake sediments, northeastern United States. *Ecotoxicology*,
740 *14*(1–2), 85–99. https://doi.org/10.1007/s10646-004-6261-2
741 Philibert, A., Prairie, Y. T., and Carcaillet, C. (2003). 1200 years of fire impact on biogeochemistry as
742 inferred from high resolution diatom analysis in a kettle lake from the Picea mariana-moss
743 domain (Quebec, Canada). *Journal of Paleolimnology*, *30*(2), 167–181.
744 https://doi.org/10.1023/A:1025526200880
745 Pompeani, D. P., McLauchlan, K. K., Chileen, B. V., Calder, W. J., Shuman, B. N., and Higuera, P.
746 E. (2020). The biogeochemical consequences of late Holocene wildfires in three subalpine lakes
747 from northern Colorado. *Quaternary Science Reviews*, *236*, 106293.
748 https://doi.org/10.1016/j.quascirev.2020.106293
749 Pretty, T. J., Chanyi, C.-M., Kuhn, C., and Gray, D. K. (2020). Factors influencing the structure of
750 macroinvertebrate communities in subarctic lakes affected by wildfires. *Canadian Journal of*
751 *Fisheries and Aquatic Sciences*. https://doi.org/10.1139/cjfas-2020-0141
752 Prince, T. J., Pisaric, M. F. J., and Turner, K. W. (2018). Postglacial Reconstruction of Fire History
753 Using Sedimentary Charcoal and Pollen From a Small Lake in Southwest Yukon Territory,
754 Canada. *Frontiers in Ecology and Evolution*, *6*(DEC), 209.
755 https://doi.org/10.3389/fevo.2018.00209
756 Probst, A., El Gh'mari, A., Aubert, D., Fritz, B., and McNutt, R. (2000). Strontium as a tracer of
757 weathering processes in a silicate catchment polluted by acid atmospheric inputs, Strengbach,

758 France. *Chemical Geology*, *170*(1–4), 203–219. https://doi.org/10.1016/S0009-2541(99)00248-X
759 Rhoades, C. C., Chow, A. T., Covino, T. P., Fegel, T. S., Pierson, D. N., and Rhea, A. E. (2019). The
760 Legacy of a Severe Wildfire on Stream Nitrogen and Carbon in Headwater Catchments.
761 *Ecosystems*, *22*(3), 643–657. https://doi.org/10.1007/s10021-018-0293-6
762 Roberts, S. L., Kirk, J. L., Muir, D. C. G., Wiklund, J. A., Evans, M. S., Gleason, A., et al. (2021).
763 Quantification of Spatial and Temporal Trends in Atmospheric Mercury Deposition across
764 Canada over the Past 30 Years. *Environmental Science and Technology*, *55*(23), 15766–15775.
765 https://doi.org/10.1021/ACS.EST.1C04034
766 Sae-Lim, J., Russell, J. M., Vachula, R. S., Holmes, R. M., Mann, P. J., Schade, J. D., and Natali, S. M.
767 (2019). Temperature-controlled tundra fire severity and frequency during the last millennium in
768 the Yukon-Kuskokwim Delta, Alaska: *Https://Doi.Org/10.1177/0959683619838036*.
769 https://doi.org/10.1177/0959683619838036
770 Sanei, H., and Goodarzi, F. (2006). Relationship between organic matter and mercury in recent lake
771 sediment: The physical–geochemical aspects. *Applied Geochemistry*, *21*(11), 1900–1912.
772 https://doi.org/10.1016/j.apgeochem.2006.08.015
773 Sanei, H., Outridge, P. M., Dallimore, A., and Hamilton, P. B. (2010). Mercury–organic matter
774 relationships in pre-pollution sediments of thermokarst lakes from the Mackenzie River Delta,
775 Canada: the role of depositional environment. *Biogeochemistry*, *107*(1–3), 149–164.
776 https://doi.org/10.1007/s10533-010-9543-1
777 Shakesby, R. A. (2011). Post-wildfire soil erosion in the Mediterranean: Review and future research
778 directions. *Earth-Science Reviews*, *105*(3), 71–100.
779 https://doi.org/10.1016/j.earscirev.2011.01.001
780 Shotyk, W., Appleby, P. G., Bicalho, B., Davies, L., Froese, D., Grant-Weaver, I., et al. (2016). Peat
781 bogs in northern Alberta, Canada reveal decades of declining atmospheric Pb contamination.

Geophysical Research Letters, *43*(18), 9964–9974. https://doi.org/10.1002/2016GL070952

Spencer, C. N., Gabel, K. O., and Hauer, F. R. (2003). Wildfire effects on stream food webs and nutrient dynamics in Glacier National Park, USA. *Forest Ecology and Management*, *178*(1), 141–153. https://doi.org/10.1016/S0378-1127(03)00058-6

Stevens-Rumann, C. S., and Morgan, P. (2019, December 1). Tree regeneration following wildfires in the western US: a review. *Fire Ecology*. SpringerOpen. https://doi.org/10.1186/s42408-019-0032-1

Strode, S. A., Jaeglé, L., Jaffe, D. A., Swartzendruber, P. C., Selin, N. E., Holmes, C., and Yantosca, R. M. (2008). Trans-Pacific transport of mercury. *Journal of Geophysical Research: Atmospheres*, *113*(D15), D15305. https://doi.org/10.1029/2007JD009428

Tsui, M. T. K., Blum, J. D., and Kwon, S. Y. (2020). Review of stable mercury isotopes in ecology and biogeochemistry. *Science of The Total Environment*, *716*, 135386. https://doi.org/10.1016/J.SCITOTENV.2019.135386

Turner, M. G., Braziunas, K. H., Hansen, W. D., and Harvey, B. J. (2019). Short-interval severe fire erodes the resilience of subalpine lodgepole pine forests. *Proceedings of the National Academy of Sciences of the United States of America*, *166*(23), 11319–11328. https://doi.org/10.1073/pnas.1902841116

Waters, M. N., Metz, A. P., Smoak, J. M., and Turner, H. (2019). Chronic prescribed burning alters nutrient deposition and sediment stoichiometry in a lake ecosystem. *Ambio*, *48*(6), 672–682. https://doi.org/10.1007/s13280-018-1094-z

Webster, J. P., Kane, T. J., Obrist, D., Ryan, J. N., and Aiken, G. R. (2016). Estimating mercury emissions resulting from wildfire in forests of the Western United States. *Science of the Total Environment*, *568*, 578–586. https://doi.org/10.1016/j.scitotenv.2016.01.166

Wiklund, J. A., Kirk, J. L., Muir, D. C. G., Evans, M., Yang, F., Keating, J., and Parsons, M. T.

(2017). Anthropogenic mercury deposition in Flin Flon Manitoba and the Experimental Lakes Area Ontario (Canada): A multi-lake sediment core reconstruction. *Science of the Total Environment*, *586*, 685–695. https://doi.org/10.1016/j.scitotenv.2017.02.046

Wildland Fire Management, G. of Y. (2014). Fire History. *Geoportal*. Wildland Fire Management, Government of Yukon. Retrieved from https://geoweb.gov.yk.ca/geoportal/catalog/search/resource/details.page?uuid=%7B26A4B563-B9DD-4C6C-BB17-FD805B7799AF%7D

Wu, L., Taylor, M. P., and Handley, H. K. (2017). Remobilisation of industrial lead depositions in ash during Australian wildfires. *Science of The Total Environment*, *599–600*, 1233–1240. https://doi.org/10.1016/j.scitotenv.2017.05.044

Xu, H., Liu, B., and Wu, F. (2010). Spatial and temporal variations of Rb/Sr ratios of the bulk surface sediments in Lake Qinghai. *Geochemical Transactions 2010 11:1*, *11*(1), 1–8. https://doi.org/10.1186/1467-4866-11-3

Zabel, N. A., Hall, R. I., Branfireun, B. A., and Swanson, H. K. (2021). Mercury accumulation in sediments of Lhù'ààn Mân' (Kluane Lake, YT): Response to past hydrological change. *Https://Doi.Org/10.1080/15230430.2021.1940790*, *53*(1), 179–195. https://doi.org/10.1080/15230430.2021.1940790

Zdanowicz, C., Karlsson, P., Bekholmen, I., Roach, P., Poulain, A., Yumvihoze, E., et al. (2018). Snowmelt, glacial and atmospheric sources of mercury to a subarctic mountain lake catchment, Yukon, Canada. *Geochimica et Cosmochimica Acta*, *238*, 374–393. https://doi.org/10.1016/J.GCA.2018.06.003